

ULTRAVIOLET OBSERVATIONS OF COOL STARS. V. THE LOCAL DENSITY OF INTERSTELLAR MATTER

W. MCCLINTOCK, R. C. HENRY*†, AND H. W. MOOS*

Physics Department, The Johns Hopkins University

AND

J. L. LINSKY*‡

Joint Institute for Laboratory Astrophysics, University of Colorado and National Bureau of Standards, Boulder

Received 1975 October 24; revised 1975 December 5

ABSTRACT

A high-resolution *Copernicus* observation of the chromospheric $L\alpha$ emission line of the nearby (3.3 pc) K dwarf ϵ Eri sets limits on the velocity, the velocity dispersion, and the density n_H of atomic hydrogen in the local interstellar medium. Analysis shows that the interstellar $L\alpha$ absorption is on the flat portion of the curve of growth. An upper limit of $n_H = 0.12 \text{ cm}^{-3}$ is derived. The value of n_H is $0.08 \pm 0.04 \text{ cm}^{-3}$ if the velocity dispersion parameter $b = 9 \text{ km s}^{-1}$, corresponding to a temperature of 5000 K. Also, the interstellar deuterium $L\alpha$ line may be present in the spectrum.

Subject headings: interstellar: matter — line profiles — stars: late type

I. INTRODUCTION

Bright late-type stars have sufficient flux at $L\alpha$, and exist in sufficient numbers in the solar neighborhood, to permit study of the local (<30 pc) interstellar medium (ISM) through observation of the interstellar absorption of $L\alpha$. Such measurements are important in that the ISM may contain only one component over these short distances. To date Moos *et al.* (1974, Paper I), McClintock *et al.* (1975a, Paper III), and McClintock *et al.* (1975b, Paper IV) have studied K-type stars in this manner; Dupree (1975) has studied α Aur; and Evans, Jordan, and Wilson (1975) have studied α CMi. The results of these studies are that the K-star work indicates that only an upper limit in the range 0.1–0.2 cm^{-3} can be set for n_H , the local interstellar atomic hydrogen density, while Dupree (1975) derives 0.01 cm^{-3} and Evans, Jordan, and Wilson (1975) derive 0.015 to 0.03 cm^{-3} for the G and F stars, respectively. All of these observations were made with the low-resolution channel (U2: $\sim 0.2 \text{ \AA}$ resolution) of the Princeton spectrometer aboard the *Copernicus* satellite (Rogerson, Spitzer, *et al.* 1973).

In this *Letter* we present high-resolution (U1: $\sim 0.06 \text{ \AA}$) *Copernicus* observations of chromospheric $L\alpha$ emission in the K2 V star ϵ Eri (3.3 pc distant), and we discuss the way interstellar H I densities determined from spectra of this type depend on the models assumed for the interstellar medium and the intrinsic stellar emission line.

Because the $L\alpha$ absorption is on the flat portion of

* Guest investigator with the Princeton University telescope on the *Copernicus* satellite, which is sponsored and operated by the National Aeronautics and Space Administration.

† Alfred P. Sloan Foundation Research Fellow.

‡ Staff member, Laboratory Astrophysics Division, National Bureau of Standards.

the curve of growth, because the intrinsic stellar $L\alpha$ flux is not known, and because there are uncertainties in the physical state of the interstellar medium, we conclude that there are ambiguities in the data which permit only an upper limit (of about 0.1 cm^{-3}) for the local interstellar hydrogen density along the line of sight to ϵ Eri. Ultimately these ambiguities may be overcome with very high signal-to-noise ratio data, measurement of interstellar deuterium absorption, and a better understanding of the intrinsic stellar $L\alpha$ flux. However, ambiguities of the type discussed here must be considered for all present determinations of the local ISM hydrogen density which use the $L\alpha$ emission profile from late-type stars.

Another way of deriving the local ISM properties is to analyze the solar $L\alpha$ radiation backscattered by interstellar hydrogen flowing through the solar system (cf. Fahr 1974 for a detailed review). This work suggests that $n_H \approx 0.1 \text{ cm}^{-3}$ and $T \approx 10^3\text{--}10^4 \text{ K}$ (Thomas 1972). The magnitude of the velocity of this flow is uncertain, with values as low as 2 km s^{-1} (Bertaux, Ammar, and Blamont 1972) and as high as 20 km s^{-1} (Fahr and Lay 1972) proposed. The present data directly measure the component of this velocity along the line of sight to ϵ Eri, although not with great precision.

II. OBSERVATIONS

On 1975 January 15/16, 48 high-resolution (*Copernicus* U1 channel) scans of the H I resonance line $\lambda 1215.67$ ($L\alpha$) of ϵ Eri were obtained. Observing techniques and data reduction procedures are described in Paper III.

In Figure 1, the solid line is a histogrammed average of the scans of ϵ Eri, after subtraction of a background (due primarily to energetic particles) estimated from the "standard table of backgrounds" of Paper III. No smoothing of the data by sliding averages of adjacent

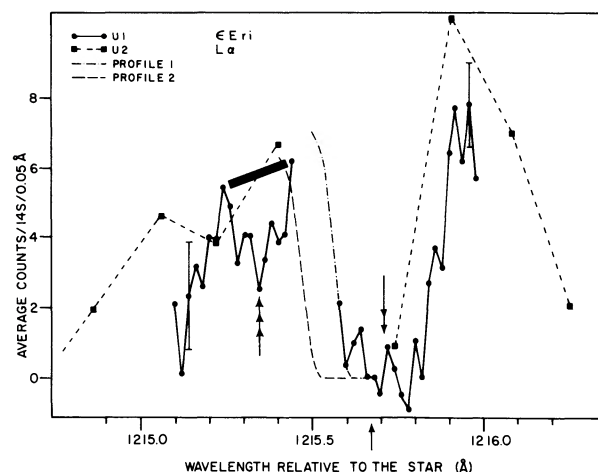


FIG. 1.—The solid line is a high-resolution *Copernicus* observation of the core of the chromospheric $\text{L}\alpha$ emission from the K2 dwarf ϵ Eri. Filled circles, data points. The interruption in the data is caused by deletion of points contaminated by geocoronal $\text{L}\alpha$ emission. Error bars are $\pm 1\sigma$. Ordinate, number of photomultiplier pulses per 14 s per resolution element per scan. Profile 1 (symmetric about $\lambda 1215.71$: double-headed arrow) and profile 2 (symmetric about $\lambda 1215.67$: single-headed arrow at nominal line center) represent two extreme interstellar absorption profiles used to interpolate the deleted points. If profile 2 is correct, the depression at $\lambda 1215.34$ is near the wavelength expected for absorption by interstellar deuterium $\text{L}\alpha$ (see text). The triple-headed arrow shows the center of the absorption dip as established by eye estimate. For comparison the low-resolution absorption of Paper IV is shown as a thin dashed line, with filled squares for the data points. All previous attempts to measure the total interstellar density by the present method have used low-resolution data.

points has been performed. The error bars are $\pm 1\sigma$, where σ is the standard error of the mean of 48 scans evaluated for each wavelength. Geocoronal $\text{L}\alpha$ completely dominates the stellar signal for four spectral steps; furthermore, independent observations indicate that two additional spectral steps are partially contaminated. These points have been deleted from the data. The zero level was established by eye estimate from the several data points at line center. The thin dashed line is the low-resolution observation from Paper IV.

The wavelength scale in Figure 1 (vacuum values in the rest frame of the star) has been corrected by $+7.5 \text{ km s}^{-1}$ in order to reproduce the known position of the geocoronal $\text{L}\alpha$ on the day of observation. The uncertainty is $\pm 7.5 \text{ km s}^{-1}$: although the position of the geocoronal $\text{L}\alpha$ can be measured to $\pm 2.5 \text{ km s}^{-1}$, changes in spacecraft pointing may cause shifts of up to $\pm 7 \text{ km s}^{-1}$ between the wavelength scale for a stellar source and a wavelength calibration determined from an extended source (York 1975). This 7.5 km s^{-1} correction is in agreement with evidence that a systematic correction $\sim +10 \text{ km s}^{-1}$ ($+0.041 \text{ \AA}$) must be applied to the U1 wavelength scale (York 1975). A single-headed arrow marks nominal line center, $\lambda 1215.67$ (corrected scale). Note that no correction has been applied to the wavelength scale of the U2 data shown in Figure 1, which may be in error by as much as 0.08 \AA . Although the nominal resolution of U1 is 0.05 \AA , spacecraft

orbital motion introduces small shifts in the wavelength scale from scan to scan. Histogramming such scans introduces a smearing in wavelength, reducing the resolution to 0.06 \AA .

This high-resolution profile is consistent with the low-resolution observations, which indicate that the shape of the emission profile is similar to the solar $\text{L}\alpha$ line (but with a slightly smaller half-width) and that the stellar surface flux on the day of observation was nearly equal to the observed value for the quiet Sun. Since the surface gravity of ϵ Eri is nearly equal to the solar value (Krishna Swamy 1966) one might expect that the amount of self-absorption present in the $\text{L}\alpha$ profile of ϵ Eri should be similar to that observed for the Sun, that is, about 30 per cent. The decline to zero intensity that may be inferred from the flatness of the line bottom in Figure 1, then, must be due to interstellar absorption.

Except for a single datum in Figure 1, geocoronal emission dominates the short-wavelength wing of the interstellar absorption component (deleted points), and no completely certain determination of the wavelength center of the interstellar absorption is possible. For the purpose of interpolating the deleted data, two extreme curves (profiles 1 and 2) which are consistent with the data are shown in Figure 1. Profile 1 (dot-dashed line) passes through the single uncontaminated datum in the short-wavelength wing of the absorption line and is symmetric about $\lambda 1215.71 \pm 0.01$ (double-headed arrow). The inferred heliocentric line-of-sight velocity for interstellar hydrogen is $+25.3 \pm 2.5 \text{ km s}^{-1}$. Profile 2 (dashed line) passes between the first two uncontaminated data points shortward of the geocoronal line and is symmetric about $\lambda 1215.67 \pm 0.01$ (nominal rest wavelength in the velocity frame of the star). The corresponding heliocentric line-of-sight velocity for the gas is $15.4 \pm 2.5 \text{ km s}^{-1}$, the same as that of the star (Allen 1973). Any wavelength between these extrema represents an absorption center consistent with the data. Including the $\pm 7.5 \text{ km s}^{-1}$ uncertainty in the absolute calibration of the U1 wavelength scale, one may infer from these two profiles a range $15.4 \pm 7.9 \text{ km s}^{-1}$ (profile 2) to $25.3 \pm 7.9 \text{ km s}^{-1}$ (profile 1) for the magnitude of the interstellar flow velocity toward ϵ Eri. Accepting the single datum shortward of line center suggests that profile 1 is correct, but $\text{L}\alpha$ backscatter analyses favor profile 2 (Fahr 1974). Furthermore, as discussed in the next paragraph, if the dip in the data near 1215.34 \AA is the result of interstellar deuterium absorption, profile 2 is again favored.

Recent measurements of the deuterium-to-hydrogen ratio in Jupiter, $\text{D}/\text{H} = 2.1 \pm 0.4 \times 10^{-5}$ (Trauger *et al.* 1973), and in the interstellar medium toward β Cen, $\text{D}/\text{H} = 1.4 \pm 0.2 \times 10^{-5}$ (Rogerson and York 1973), allow one to predict the expected amount of interstellar deuterium absorption in the spectrum of ϵ Eri. For $\text{D}/\text{H} = 1.75 \times 10^{-5}$ and $n_{\text{H}} = 0.1 \text{ cm}^{-3}$, the deuterium $\text{L}\alpha$ absorption line lies on the flat portion of the curve of growth but is not yet fully saturated; for $T = 5000 \text{ K}$ the equivalent width is $W_{\lambda} = 0.052 \text{ \AA}$. It is blueshifted by 0.329 \AA from the hydrogen $\text{L}\alpha$ line. If the dip in

Figure 1 centered at $\lambda 1215.34 \pm 0.03$ is the result of deuterium absorption, then the equivalent width estimated for a "continuum level," shown as a heavy sloping line, is 0.06 \AA , which is in good agreement with the value predicted above. Although the equivalent width for this feature is not well determined, the line center can be estimated from the symmetry of the profile with a fair degree of accuracy, and is shown by the triple arrow in Figure 1. The full width at half-maximum, $\sim 0.14 \text{ \AA}$, is too broad for an instrumental profile of 0.06 \AA and a temperature of 5000 K ; but detection of deuterium would imply that profile 2 is the correct choice. Thus, higher values of the temperature are indicated, which would lead to a broader profile. Also, it is possible that the instrumental profile is broader than 0.06 \AA in practice, because of guidance errors in repeated reobservation of a faint red star from orbit to orbit. A definitive conclusion regarding the choice of profile will be possible when we have made additional observations during a period when geocoronal $\text{L}\alpha$ does not obscure either line wing.

Also, if confirmed, this will be the first observation of the interstellar deuterium $\text{L}\alpha$ line, to our knowledge.

III. ANALYSIS

The method of analysis which we adopt is the construction of models for the intrinsic stellar emission line, and the interstellar absorption. Those models which fit the observed profile are regarded as acceptable, and those which do not are rejected. Certain assumptions must be made, namely: (a) the intrinsic stellar profile has a shape similar to the solar $\text{L}\alpha$ line (Bruner and Rense 1969), although the amount and shape of the self-absorption may be different; (b) the intrinsic stellar surface flux is within a factor 2 of the solar value; (c) the local interstellar medium along the line of sight is homogeneous and can be characterized by a single density and temperature.

Voigt profiles were used for the interstellar component. Because the intensity of the stellar $\text{L}\alpha$ emission line at the surface of the star is not known, it is not possible to determine precisely the amount of damping present in the far wings ($\geq 0.5 \text{ \AA}$) of the absorption line. Thus values of n_{H} and b , where b is $\sqrt{2}$ times the line-of-sight velocity dispersion, can only be inferred from the shape of the core—which must be determined with a high signal-to-noise ratio, as well as high spectral resolution. Detailed testing demonstrates that these conclusions are not dependent upon the specific shape chosen for the intrinsic profile, and that varying the assumed depth of the self-reversal and its overall shape has negligible effect on the values of n_{H} and b deduced. Indeed, the only critical parameter is the total stellar surface flux.

If $\Delta\lambda$ is the Doppler shift of the center of absorption from the nominal wavelength, we have seen that the data allow $\Delta\lambda = 0$ (profile 2) to $\Delta\lambda = 0.04 \text{ \AA}$ (profile 1). For both of these values, models were tested for a wide range of values of n_{H} and b . For $n_{\text{H}} \leq 0.02 \text{ cm}^{-3}$ and $b > 10 \text{ km s}^{-1}$ the shape of the absorption core is dominated by the choice of b , and very low densities

are possible for suitably large values of b ($\geq 14 \text{ km s}^{-1}$). With $n_{\text{H}} > 0.10 \text{ cm}^{-3}$ (and $\Delta\lambda = 0.04$) or for $n_{\text{H}} > 0.12 \text{ cm}^{-3}$ (and $\Delta\lambda = 0$), no values of b provided satisfactory agreement between models and the present data. Models with slightly higher values of n_{H} (say, < 0.4), while incompatible with the present data, do not severely disagree with observation and perhaps should not be considered to be absolutely excluded.

Figure 2 shows the ranges of n_{H} and b which provide satisfactory agreement between models and data. Two regions are shown, one for profile 2 and one for profile 1. Average densities have been converted to column densities (*right-hand scale*), assuming the distance to ϵ Eri to be 3.3 pc (Hoffleit 1964); and b -values have been converted to temperatures (*top scale*), assuming the velocity dispersion along the line-of-sight to be due entirely to thermal motion.

IV. DISCUSSION

The method of model fitting is not the only possible approach to the problem of determining the amount of interstellar absorption. For example, one could instead multiply the observed profile by $\exp[+\tau(\Delta\lambda)]$, where $\tau(\Delta\lambda)$ is the optical depth of atomic hydrogen at wavelength $\Delta\lambda$ from absorption line center. However, this method, which is often used for early-type stars with high signal-to-noise ratio continuum signals, may produce misleading results for late-type stars where the stellar component is a *low* signal-to-noise ratio, *narrow* emission line, and the interstellar absorption line is saturated. (See Bohlin 1975, and note that even for high signal-to-noise ratio data the profiles resulting from the multiplication process are not smooth, particularly near line center, and one must rely upon the shape of the far wings of the profile to determine the continuum

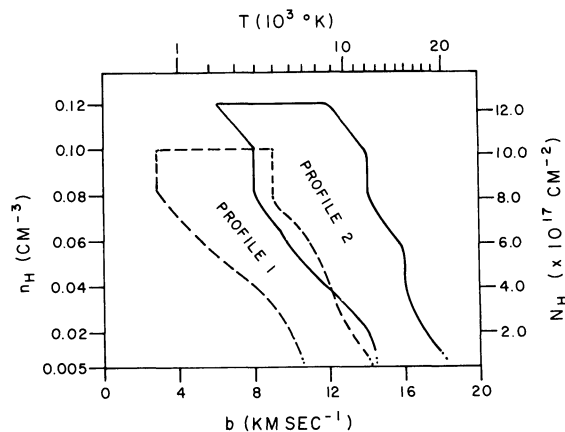


FIG. 2.—The solid line bounds the region of values of n_{H} and b which provide satisfactory agreement between models and the data for profile 2 of Fig. 1, while the heavy dashed line encloses the corresponding values for profile 1. If the dip at 1215.34 \AA in Fig. 1 is due to interstellar D, then profile 2 is favored. Left ordinate is the number density of atomic hydrogen per cubic centimeter along the line of sight, while the right-hand scale gives the column density in atoms per square centimeter. The parameter b is $\sqrt{2}$ times the line-of-sight velocity dispersion, while T is the corresponding temperature of the local interstellar medium.

level.) For the present data, lower limits for n_{H} set by this method agree with values obtained by the techniques of model fitting presented here; but estimates of upper limits for n_{H} based on this procedure resulted in values for n_{H} which are lower than those deduced from models by as much as a factor of 2. *Low-resolution* observations of the $\text{L}\alpha$ profile in nearby F and G stars have been made by Evans, Jordan, and Wilson (1975) and Dupree (1975), who have deduced extremely low line-of-sight atomic-hydrogen densities ($\sim 0.01 \text{ cm}^{-3}$). Their results were obtained by multiplying the observed profiles by $\exp [+ \tau(\Delta\lambda)]$ to obtain a suitable intrinsic profile. They also assume that the interstellar $\text{L}\alpha$ absorption line is on the damping portion of the curve of growth so that the Doppler broadening term b does not enter.

In Papers I and III it was shown that ambiguities exist in the low-resolution observations of K-type giant stars which allow only limits of $0.02 \text{ cm}^{-3} \leq n_{\text{H}} \leq 0.15 \text{ cm}^{-3}$ for line-of-sight densities to two nearby stars, α Boo (11.0 pc) and β Gem (10.8 pc). The present high-resolution observation of a nearby K dwarf shows that the data will tolerate line-of-sight values of n_{H} as high as 0.12 cm^{-3} and that the very low densities ($< 0.01 \text{ cm}^{-3}$) are unlikely unless large b values are permitted ($b \approx 14 \text{ km s}^{-1}$). If $b = 9 \text{ km s}^{-1}$, which is a reasonable value (Rogerson and York 1973), then $n_{\text{H}} = 0.08 \pm 0.04 \text{ cm}^{-3}$.

Determinations of density and temperature using the present model-fitting method are consistent with the results of $\text{L}\alpha$ sky background models, for which $n_{\text{H}} \approx 0.1 \text{ cm}^{-3}$ and $T = (7 \pm 2) \times 10^3 \text{ K}$ are considered most probable (Fahr 1974), although the present data do not exclude much lower densities with correspondingly higher temperatures.

V. CONCLUSION

The present observation of $\text{L}\alpha$ emission from ϵ Eri, with modeling of the ISM absorption, provides an upper limit to the average density of atomic hydrogen along the line of sight to this nearby K dwarf. The limit can be improved with higher signal-to-noise spectra; however, because the interstellar profile is saturated and the intrinsic stellar surface flux is not known, precise values for density and temperature will be difficult to establish without dramatic improvements in the signal-to-noise ratio of the data. If deuterium absorption is observable, it should be near the linear part of the curve of growth and it will provide an additional measure of the interstellar atomic hydrogen density.

Reasonably accurate velocity determinations result from high-resolution observations of interstellar absorption profiles, and these may prove useful in establishing the vector velocity for the local interstellar medium, independent of solar $\text{L}\alpha$ scattering models.

We wish to acknowledge support by the National Aeronautics and Space Administration to the Johns Hopkins University and the University of Colorado and important discussions with T. Holzer, A. Hundhausen, B. Savage, and D. York.

Note added in proof.—A second observation of ϵ Eri has been made (McClintock *et al.* 1975c) which clearly shows that profile 2 is correct, and also that the interstellar deuterium line is present. Thus, the interstellar hydrogen systematic velocity is $15.4 \pm 7.9 \text{ km s}^{-1}$, and its density is $\sim 0.1 \text{ cm}^{-3}$.

REFERENCES

- Allen, C. W. 1973, *Astrophysical Quantities* (London: Athlone Press).
- Bertaux, J. L., Ammar, A., and Blamont, J. E. 1972, *Space Res.*, **12**, 1559.
- Bohlin, R. C. 1975, *Ap. J.*, **200**, 402.
- Bruner, E. C., Jr., and Rense, W. A. 1969, *Ap. J.*, **157**, 417.
- Dupree, A. K. 1975, *Ap. J. (Letters)*, **200**, L27.
- Evans, R. G., Jordan, C., and Wilson, R. 1975, *Nature*, **253**, 612.
- Fahr, H. J. 1974, *Space Sci. Rev.*, **15**, 483.
- Fahr, H. J., and Lay, G. 1972, in *Mittg. der Astron. (Vienna: Gesellschaft)*.
- Hoffeit, D. 1964, *Catalogue of Bright Stars* (New Haven: Yale Univ. Observatory).
- Krishna Swamy, K. S. 1966, *Ap. J.*, **145**, 174.
- McClintock, W., Linsky, J. L., Henry, R. C., Moos, H. W., and Gerola, H. 1975a, *Ap. J.*, **202**, 165 (Paper III).
- McClintock, W., Henry, R. C., Moos, H. W., and Linsky, J. L. 1975b, *Ap. J.*, **202**, 733 (Paper IV).
- . 1975c, *Bull. AAS*, **7**, 547.
- Moos, H. W., Linsky, J. L., Henry, R. C., and McClintock, W. 1974, *Ap. J. (Letters)*, **188**, L93 (Paper I).
- Rogerson, J. B., Spitzer, L., Drake, J. F., Dressler, K., Jenkins, E. B., Morton, D. C., and York, D. G. 1973, *Ap. J. (Letters)*, **181**, L97.
- Rogerson, J. B., and York, D. G. 1973, *Ap. J. (Letters)*, **186**, L95.
- Thomas, G. E. 1972, NASA SP-308, 668.
- Trauger, J. T., Roesler, F. L., Carleton, N. P., and Traub, W. A. 1973, *Ap. J. (Letters)*, **184**, L137.
- York, D. G. 1975, *Ap. J. (Letters)*, **196**, L103.

R. C. HENRY, W. McCLINTOCK, and H. W. MOOS: Department of Physics, Homewood Campus, The Johns Hopkins University, Baltimore, MD 21218

J. L. LINSKY: Joint Institute for Laboratory Astrophysics, University of Colorado, Boulder, CO 80302